

Free-fall drop test with interchangeable surfaces to recreate concussive ice hockey head impacts

HAID, Daniel, DUNCAN, O., HART, J. and FOSTER, Leon
<<http://orcid.org/0000-0002-1551-0316>>

Available from Sheffield Hallam University Research Archive (SHURA) at:
<https://shura.shu.ac.uk/31863/>

This document is the Supplemental Material

Citation:

HAID, Daniel, DUNCAN, O., HART, J. and FOSTER, Leon (2023). Free-fall drop test with interchangeable surfaces to recreate concussive ice hockey head impacts. Sports Engineering, 26 (1): 25. [Article]

Copyright and re-use policy

See <http://shura.shu.ac.uk/information.html>

Free-fall drop test with interchangeable surfaces to recreate concussive ice hockey head impacts - Supplementary Materials

Sports Engineering - Topical Collection ISEA 2022: The 14th Conference of the International Sports Engineering Association

1. Helmet models

The helmets were chosen to represent the available price range and different liner material and design features (Fig. S1).



Fig. S1 Helmet shells and liner systems for helmet (a - d) 1, (e - h) 2, (i - l) 3, (m - p) 4, and (q - t) 5

2. Test method reliability

Mean values, standard deviations (SD), and intra-class correlation (ICC) coefficients with their respective 95% confidence intervals (CI) were calculated for flat surface peak linear acceleration (PLA) and duration (D), and oblique surface PLA, peak angular acceleration (PAA) and D to assess the test methods reliability. Values were obtained for only helmeted impacts (Table S1) and with unhelmeted impacts included (Table S2). Additional reliability values were obtained with the data grouped by impact surface.

Table S1 Mean values, SD, ICC coefficients and their respective 95% CI for flat surface PLA and D, and oblique surface PLA, PAA, and D grouped by impact surface. Unhelmeted impacts were excluded in the calculations of the ICC values.

	Mean (\pm SD)	ICC coefficient	95% Confidence Interval
Flat, PLA [g]	70.6 (\pm 28.1)	0.995	0.991 \rightarrow 0.997
96 mm	42.9 (\pm 2.3)	0.950	0.882 \rightarrow 0.982
72 mm	48.9 (\pm 2.7)	0.960	0.902 \rightarrow 0.986
48 mm	60.5 (\pm 5.2)	0.952	0.887 \rightarrow 0.982
24 mm	89.8 (\pm 11.8)	0.954	0.886 \rightarrow 0.983
MEP	111.0 (\pm 20.5)	0.969	0.911 \rightarrow 0.989
Flat, D [ms]	22.1 (\pm 6.3)	0.996	0.994 \rightarrow 0.997
96 mm	29.4 (\pm 1.2)	0.939	0.854 \rightarrow 0.978
72 mm	27.2 (\pm 1.0)	0.897	0.747 \rightarrow 0.963
48 mm	23.7 (\pm 1.1)	0.954	0.890 \rightarrow 0.983
24 mm	17.5 (\pm 1.3)	0.891	0.744 \rightarrow 0.960
MEP	12.9 (\pm 1.7)	0.838	0.619 \rightarrow 0.941
Oblique, PLA [g]	38.3 (\pm 13.2)	0.991	0.987 \rightarrow 0.994
72 mm	26.8 (\pm 3.0)	0.987	0.972 \rightarrow 0.994
48 mm	35.3 (\pm 5.6)	0.985	0.971 \rightarrow 0.993
24 mm	52.8 (\pm 11.4)	0.969	0.939 \rightarrow 0.985
Oblique, PAA [krad/s ²]	2.66 (\pm 1.10)	0.997	0.995 \rightarrow 0.998
72 mm	1.72 (\pm 0.37)	0.987	0.975 \rightarrow 0.994
48 mm	2.39 (\pm 0.62)	0.994	0.988 \rightarrow 0.997
24 mm	3.89 (\pm 0.81)	0.989	0.979 \rightarrow 0.995
Oblique, D [ms]	25.1 (\pm 5.5)	0.990	0.984 \rightarrow 0.993
72 mm	31.3 (\pm 1.8)	0.865	0.739 \rightarrow 0.936
48 mm	25.6 (\pm 1.7)	0.915	0.800 \rightarrow 0.963
24 mm	18.5 (\pm 1.6)	0.918	0.840 \rightarrow 0.961

Table S2 Mean values, standard deviations (SD), ICC coefficients and their respective 95% CI for flat surface PLA and D, and oblique surface PLA, PAA, and D grouped by impact surface. Unhelmeted impacts were included in the calculations of the ICC values.

	Mean (\pm SD)	ICC coefficient	95% Confidence Interval
Flat, PLA [g]	80.2 (\pm 49.2)	0.995	0.993 \rightarrow 0.996
96 mm	43.8 (\pm 3.1)	0.952	0.895 \rightarrow 0.981
72 mm	49.8 (\pm 3.3)	0.978	0.951 \rightarrow 0.991
48 mm	63.1 (\pm 7.5)	0.980	0.956 \rightarrow 0.992
24 mm	109.4 (\pm 46.6)	0.997	0.994 \rightarrow 0.999
MEP	135.2 (\pm 58.6)	0.984	0.965 \rightarrow 0.994
Flat, D [ms]	21.6 (\pm 6.7)	0.997	0.996 \rightarrow 0.998
96 mm	29.2 (\pm 1.3)	0.957	0.905 \rightarrow 0.983
72 mm	26.9 (\pm 1.2)	0.935	0.849 \rightarrow 0.974
48 mm	23.2 (\pm 1.5)	0.976	0.945 \rightarrow 0.990
24 mm	16.6 (\pm 2.3)	0.974	0.943 \rightarrow 0.989
MEP	11.9 (\pm 2.8)	0.957	0.906 \rightarrow 0.982
Oblique, PLA [g]	41.4 (\pm 19.7)	0.996	0.994 \rightarrow 0.997
72 mm	27.2 (\pm 3.1)	0.977	0.956 \rightarrow 0.988
48 mm	36.0 (\pm 6.1)	0.988	0.978 \rightarrow 0.994
24 mm	61.1 (\pm 22.4)	0.992	0.986 \rightarrow 0.996
Oblique, PAA [krad/s ²]	2.86 (\pm 1.42)	0.998	0.997 \rightarrow 0.998
72 mm	1.78 (\pm 0.42)	0.987	0.976 \rightarrow 0.993
48 mm	2.49 (\pm 0.70)	0.994	0.989 \rightarrow 0.997
24 mm	4.31 (\pm 1.42)	0.995	0.992 \rightarrow 0.998
Oblique, D [ms]	24.6 (\pm 5.8)	0.992	0.988 \rightarrow 0.994
72 mm	30.9 (\pm 2.0)	0.885	0.789 \rightarrow 0.941
48 mm	25.2 (\pm 1.8)	0.939	0.874 \rightarrow 0.971
24 mm	17.7 (\pm 2.3)	0.970	0.945 \rightarrow 0.985

3. Acceleration vs. time data

2.1 Flat impact surface

Linear acceleration vs. time data show a single peak for the three impact sites Front (Fig. S2), Rear (Fig. S3), and Side (Fig. S4) onto all 5 surfaces (only 96 mm, 48 mm and MEP pad shown in the manuscript). Peak accelerations decreased and impact durations increased with increasing impact surface compliance for all three impact sites.

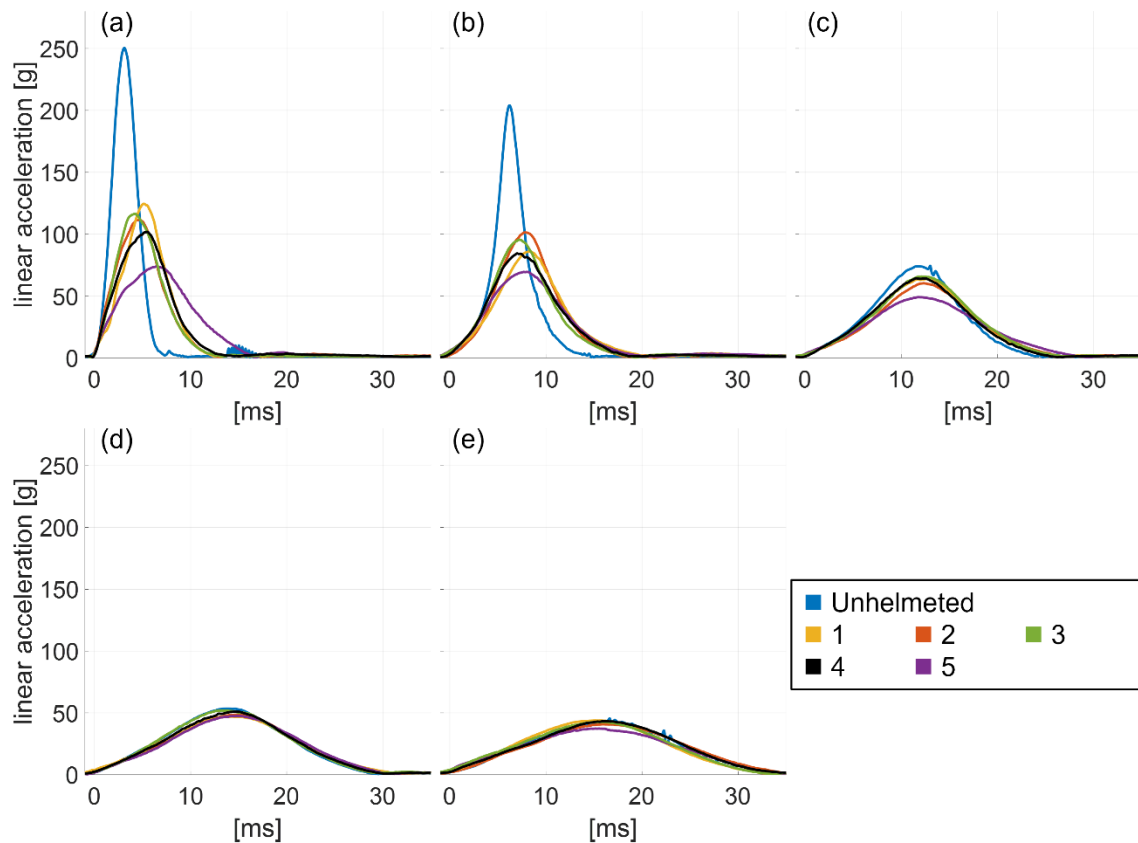


Fig. S2 Linear acceleration vs. time traces for flat surface, Front site impacts onto the (a) MEP Pad, (b) 24 mm foam layer, (c) 48 mm foam layer, (d) 72 mm foam layer, and (e) 96 mm foam layer

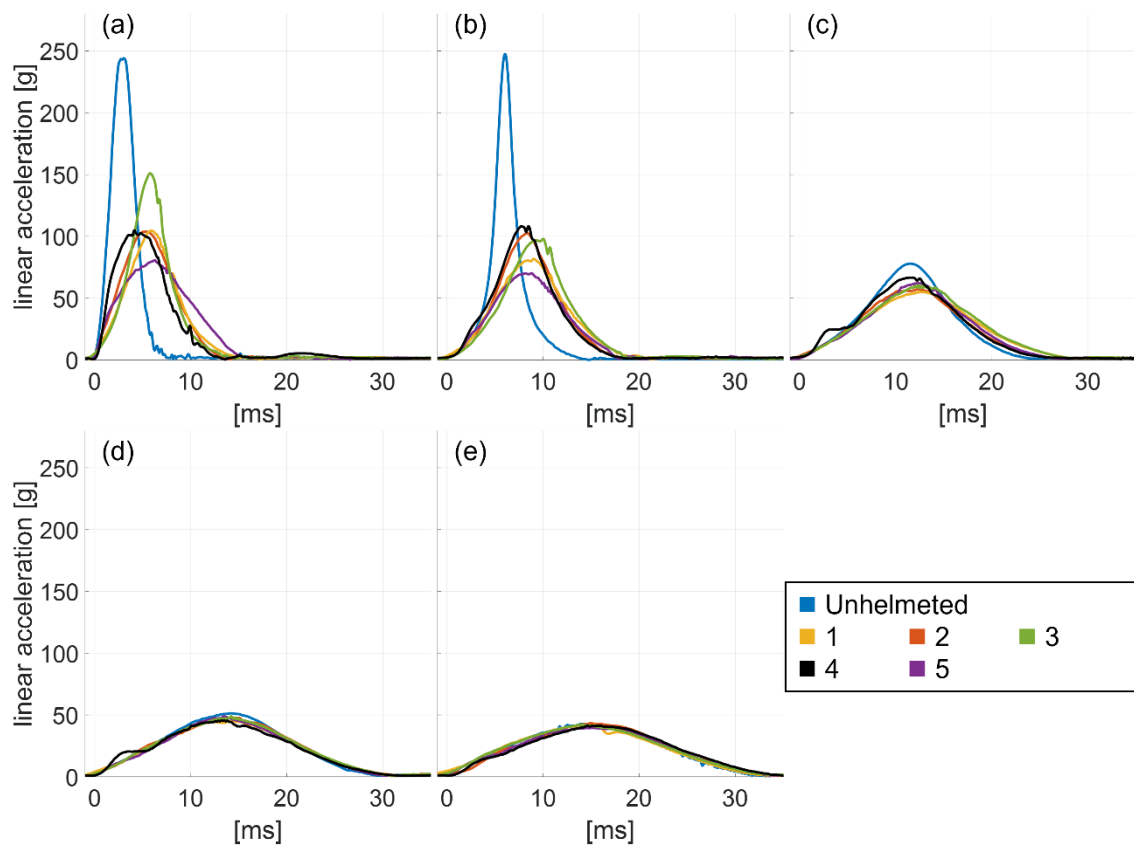


Fig. S3 Linear acceleration vs. time traces for flat surface, Rear site impacts onto the (a) MEP Pad, (b) 24 mm foam layer, (c) 48 mm foam layer, (d) 72 mm foam layer, and (e) 96 mm foam layer

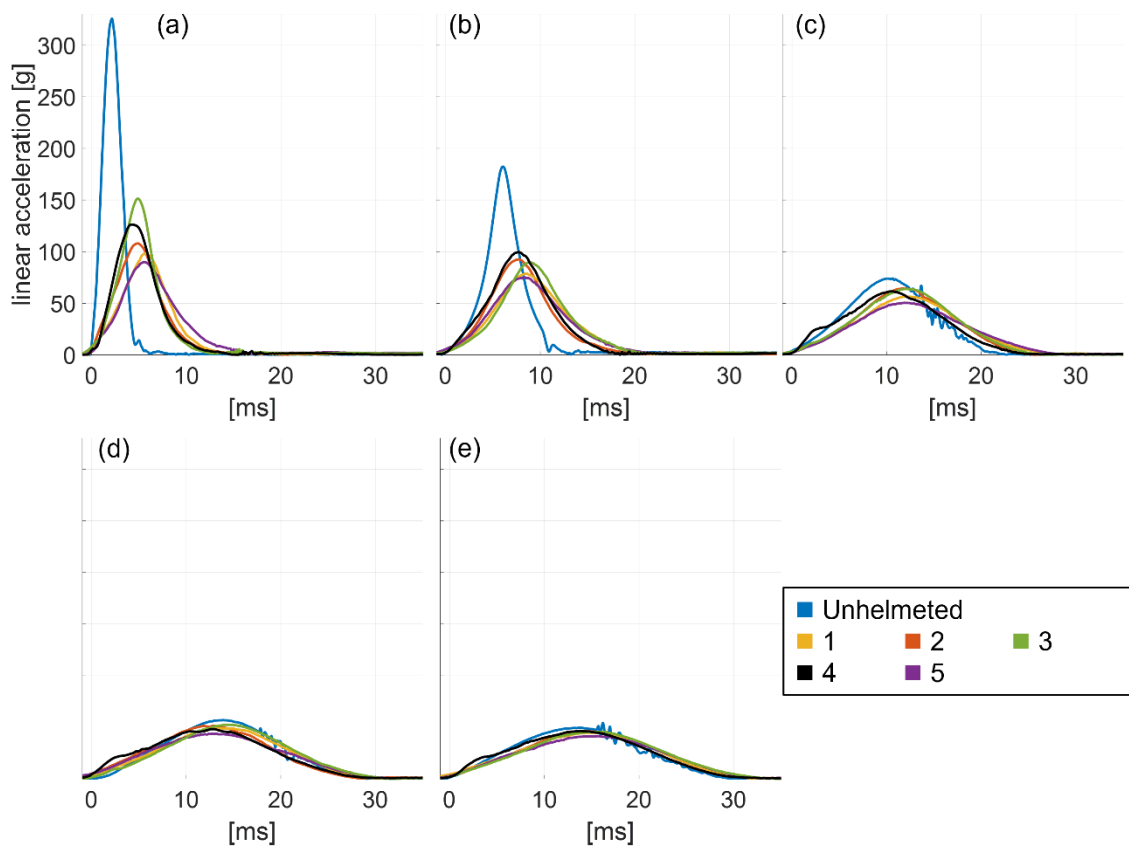


Fig. S4 Linear acceleration vs. time traces for flat surface, Side site impacts onto the (a) MEP Pad, (b) 24 mm foam layer, (c) 48 mm foam layer, (d) 72 mm foam layer, and (e) 96 mm foam layer

2.2 Oblique Impact Surface

Linear and angular acceleration vs. time data show a single peak for the additional four impact sites FrontBoss (Fig. S5), RearBoss (Fig. S6), Rear (Fig. S7), and Side (Fig. S8) onto all three surfaces, as seen for impacts onto the front site in the manuscript. Peak accelerations decreased and impact durations also increased with increasing impact surface compliance for all five impact sites.

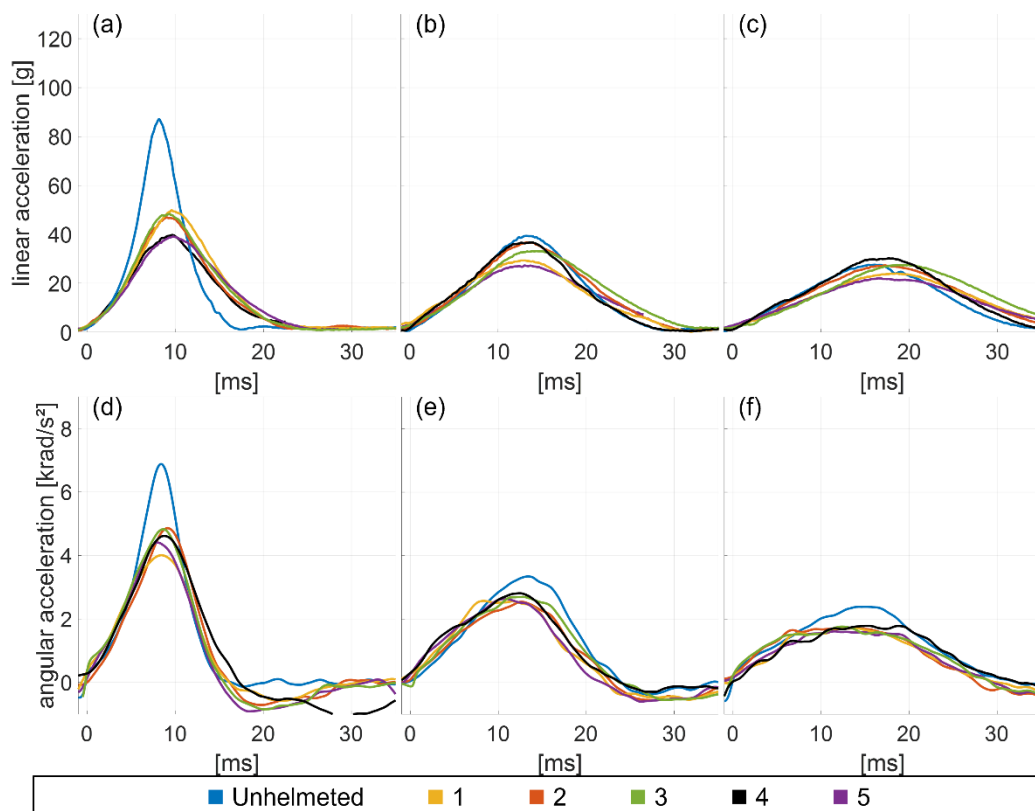


Fig. S5 (a - c) Linear and (d - f) angular acceleration vs. time traces for oblique surface, FrontBoss site impacts onto the (a & d) 24 mm foam layer, (b & e) 48 mm foam layer, and (c & f) 72 mm foam layer

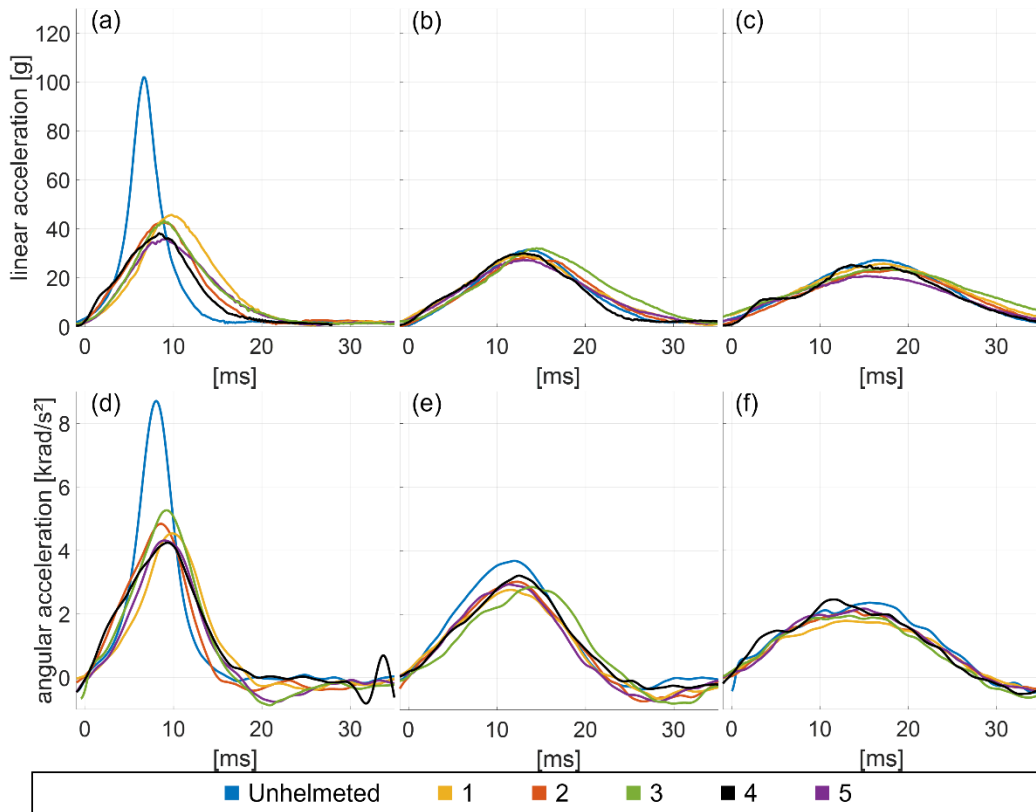


Fig. S6 (a - c) Linear and (d - f) angular acceleration vs. time traces for oblique surface, RearBoss site impacts onto the (a & d) 24 mm foam layer, (b & e) 48 mm foam layer, and (c & f) 72 mm foam layer

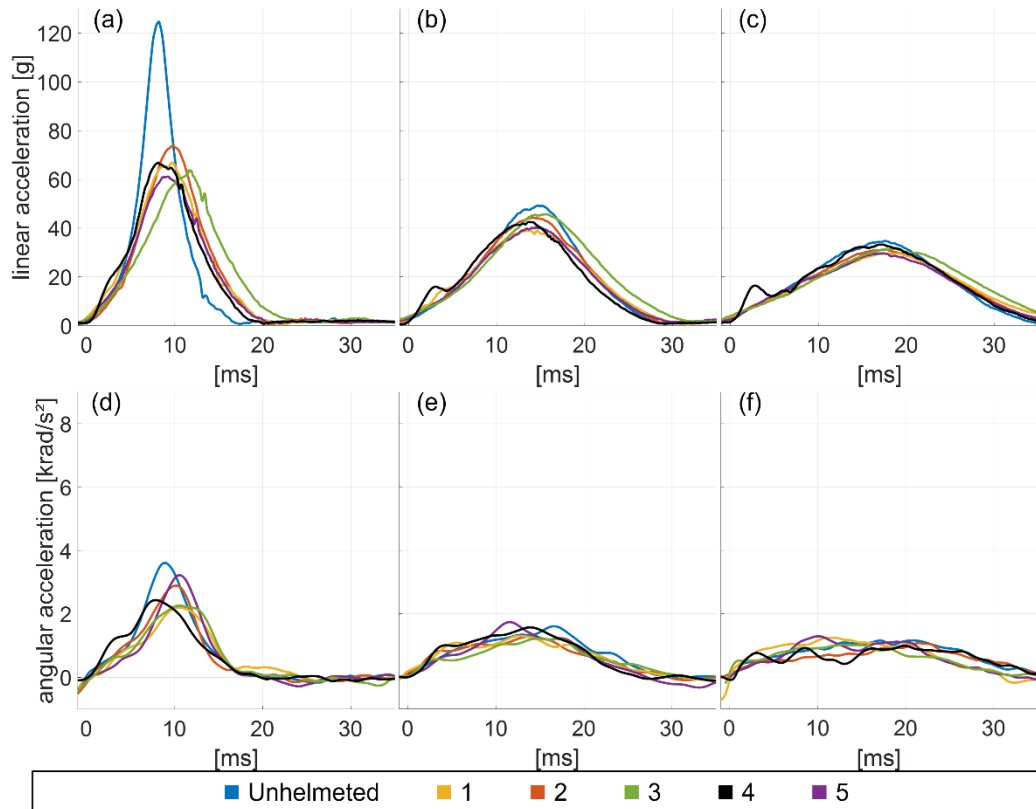


Fig. S7 (a - c) Linear and (d - f) angular acceleration vs. time traces for oblique surface, Rear site impacts onto the (a & d) 24 mm foam layer, (b & e) 48 mm foam layer, and (c & f) 72 mm foam layer

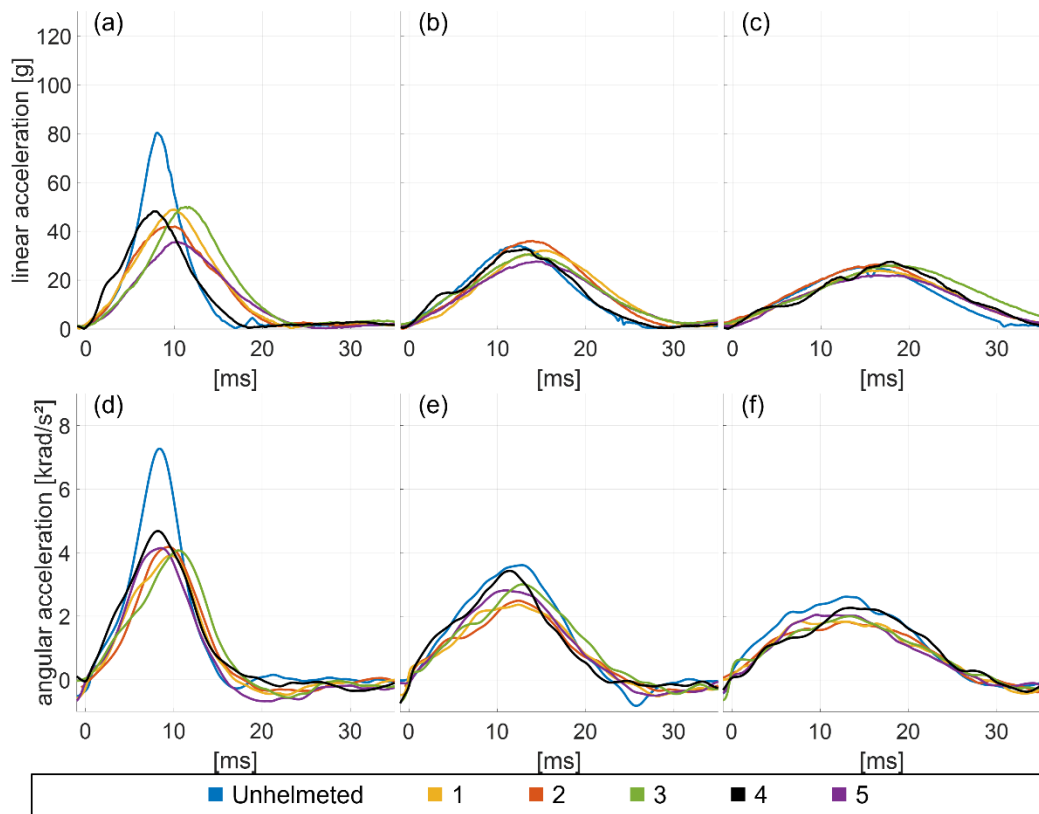


Fig. S8 (a - c) Linear and (d - f) angular acceleration vs. time traces for oblique surface, Side site impacts onto the (a & d) 24 mm foam layer, (b & e) 48 mm foam layer, and (c & f) 72 mm foam layer

4. Collated data

3.1 Flat Impact Surface

Broadly similar trends to those in the manuscript were seen between linear (Fig. S9 & Fig. S13) and angular (Fig. S14) peak accelerations, between tested helmets for the different surface compliances during flat (Fig. S9) and oblique (Fig. S13 & Fig. S14) surface impacts. Helmets increased impact duration for all compliances and impact sites (Fig. S10 & Fig. S15). The proportion of time to peak (TTP) and rebound time (RT) increased with increasing surface compliance (Fig. S11 & Fig. S16). The HIC (Fig. S12 & Fig. S17) and the RIC (Fig. S18) obtained similar trends as peak accelerations with more distinguishable differences between individual helmets.

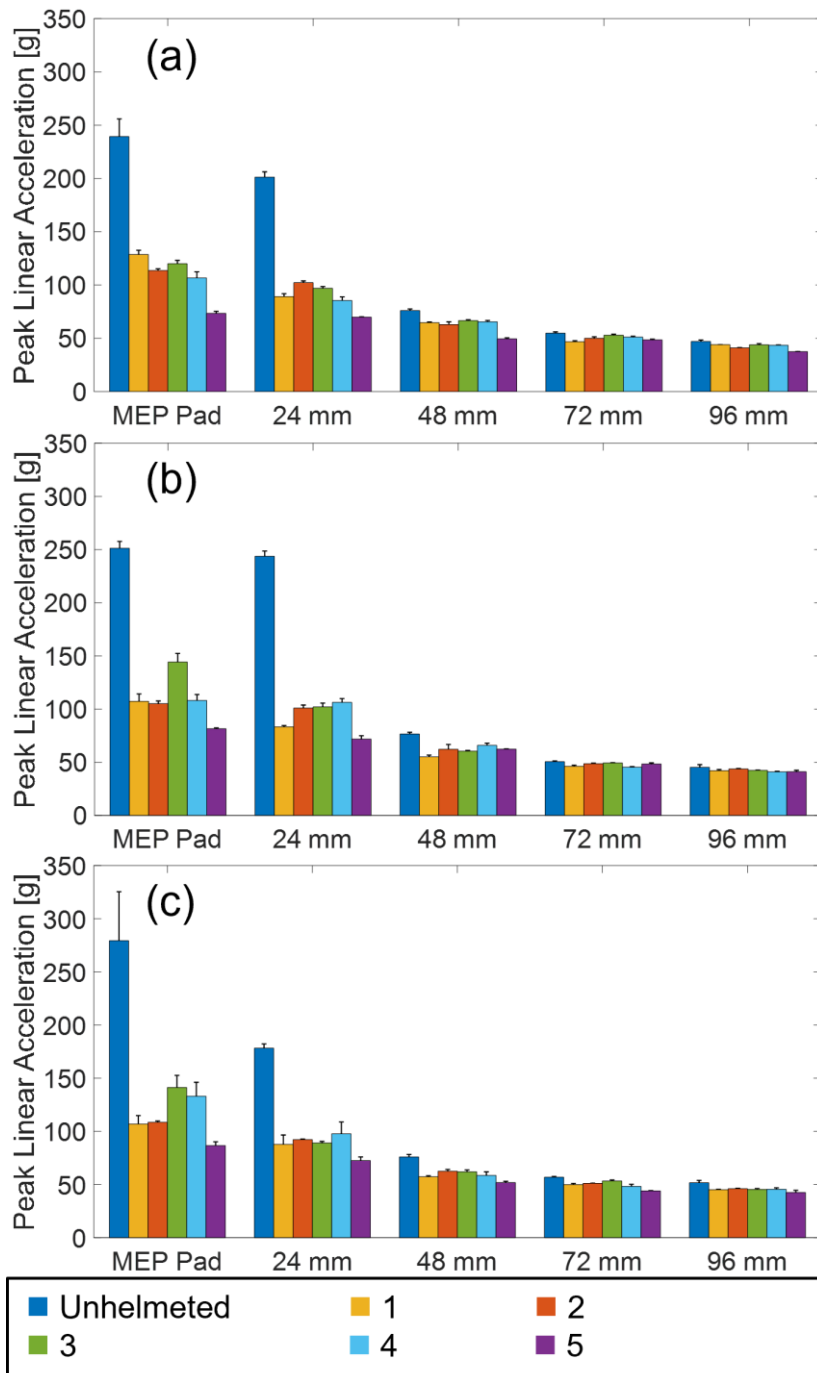


Fig. S9 Mean peak linear accelerations for all flat surface, (a) Front, (b) Rear, and (c) Side site impacts

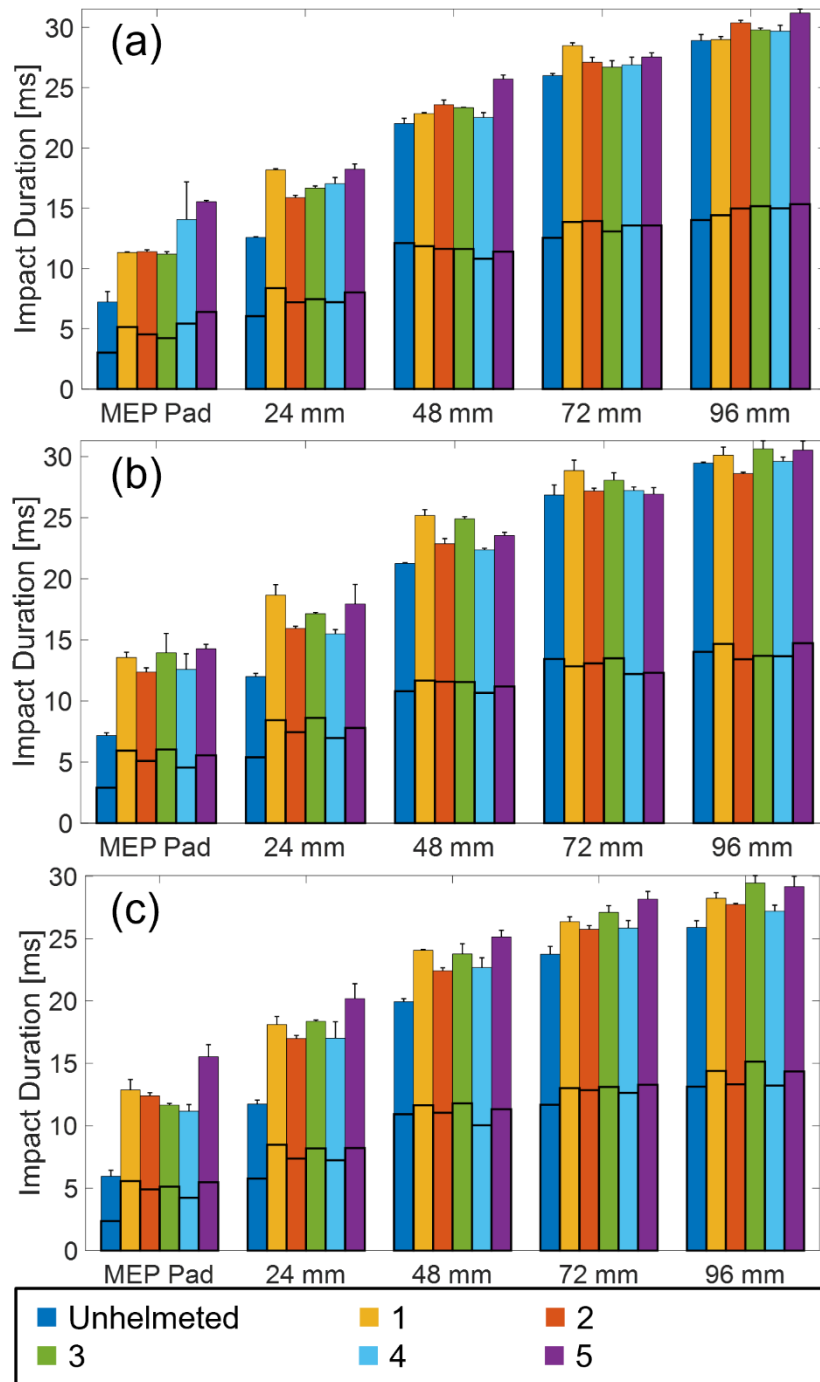


Fig. S10 Mean impact durations with horizontal bars indicating the proportion of time to peak (bottom half) and rebound time (top half) for all flat surface, (a) Front, (b) Rear, and (c) Side site impacts

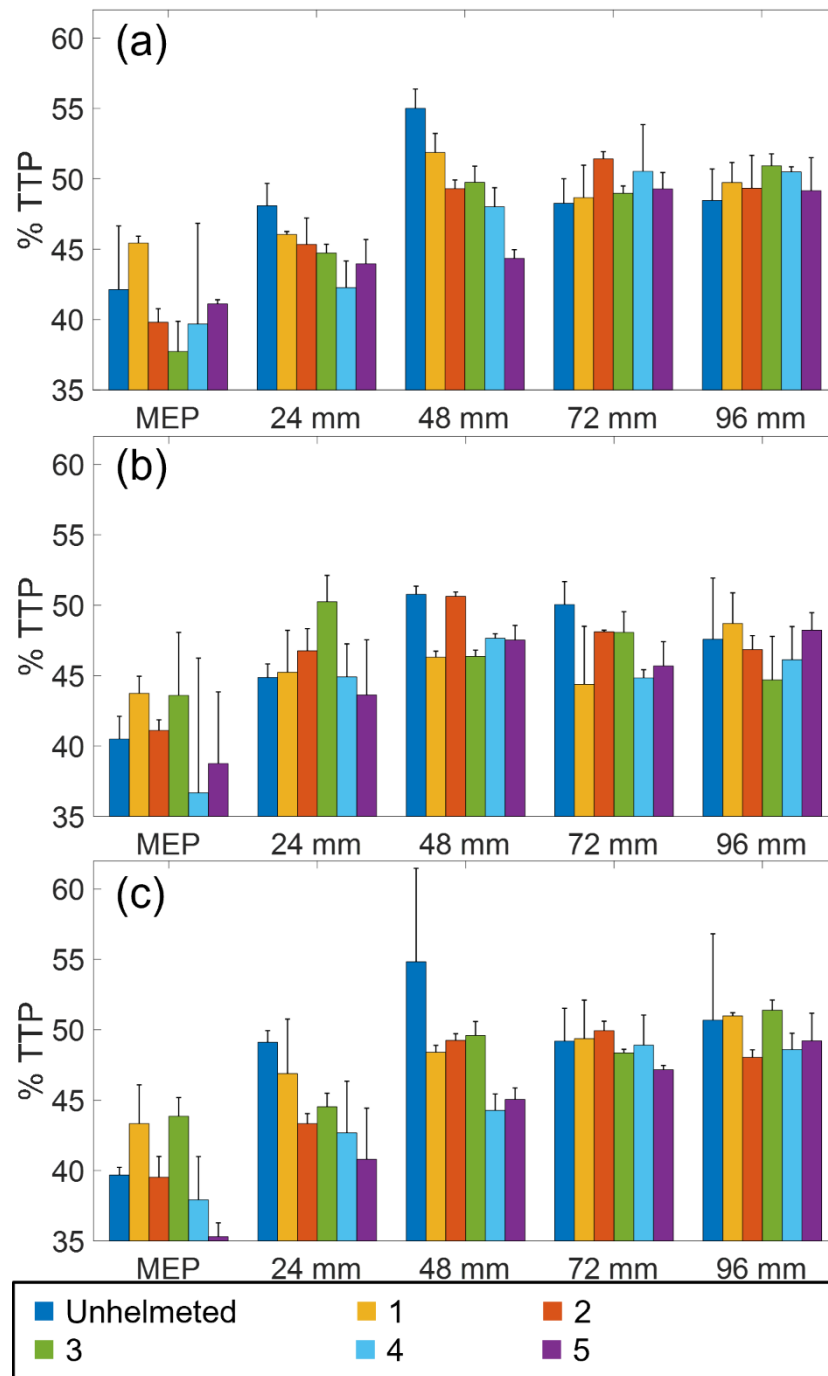
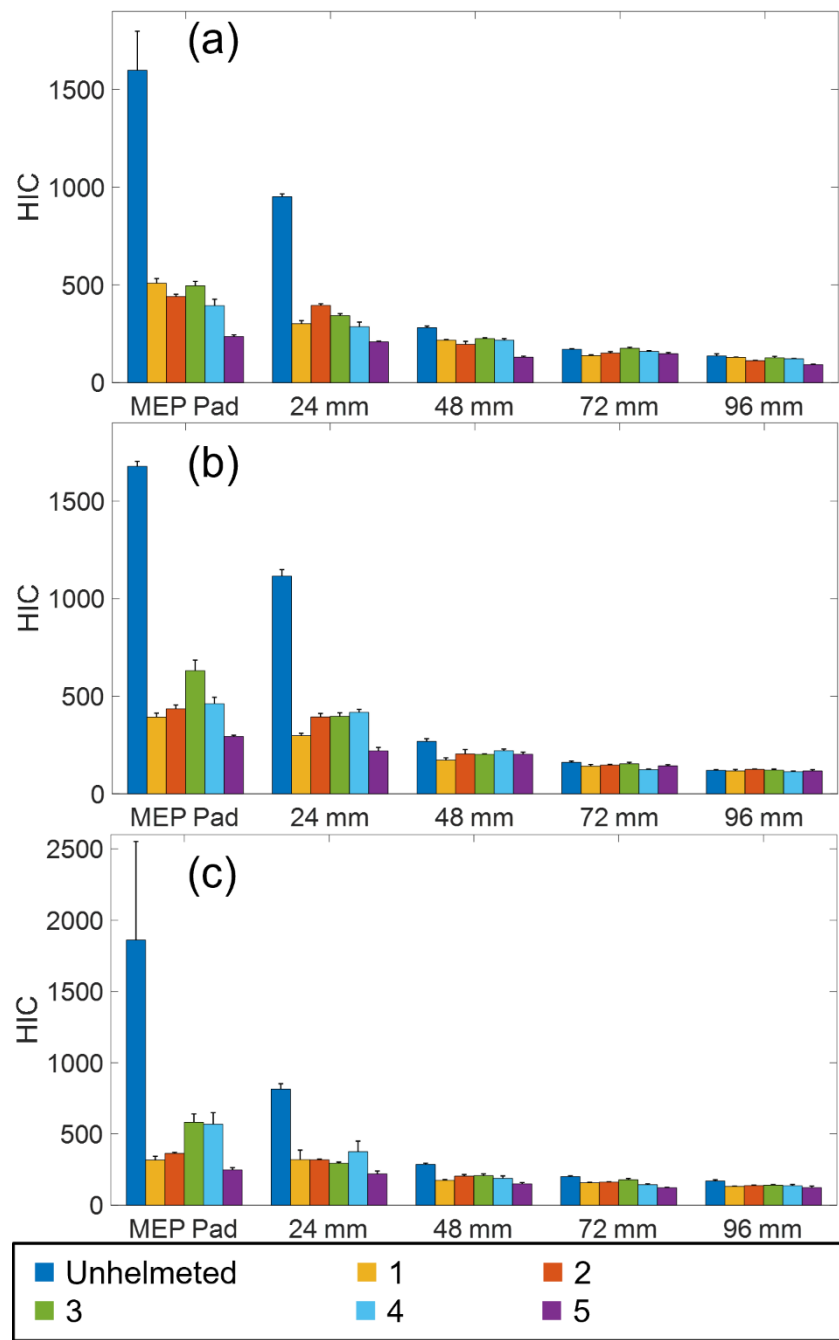


Fig. S11 Mean percentage of time to peak of the total impact duration for all flat surface, (a) Front, (b) Rear, and (c) Side site impacts



79

80 **Fig. S12** Mean HIC for all flat surface, (a) Front, (b) Rear, and (c) Side site impacts

3.2 Oblique Impact Surface

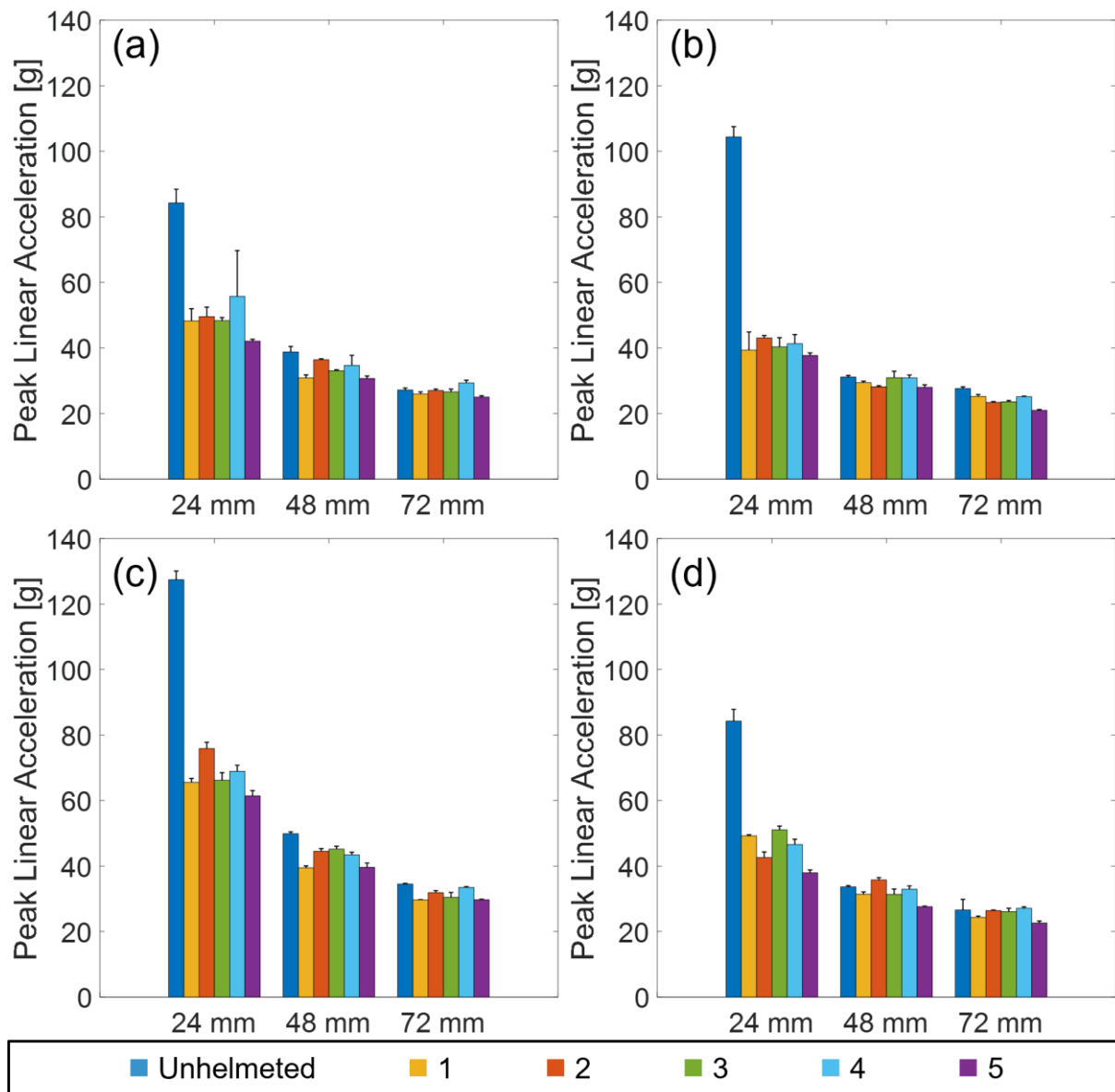


Fig. S13 Mean peak linear accelerations for all oblique surface, (a) FrontBoss, (b) RearBoss, (c) Rear, and (d) Side site impacts

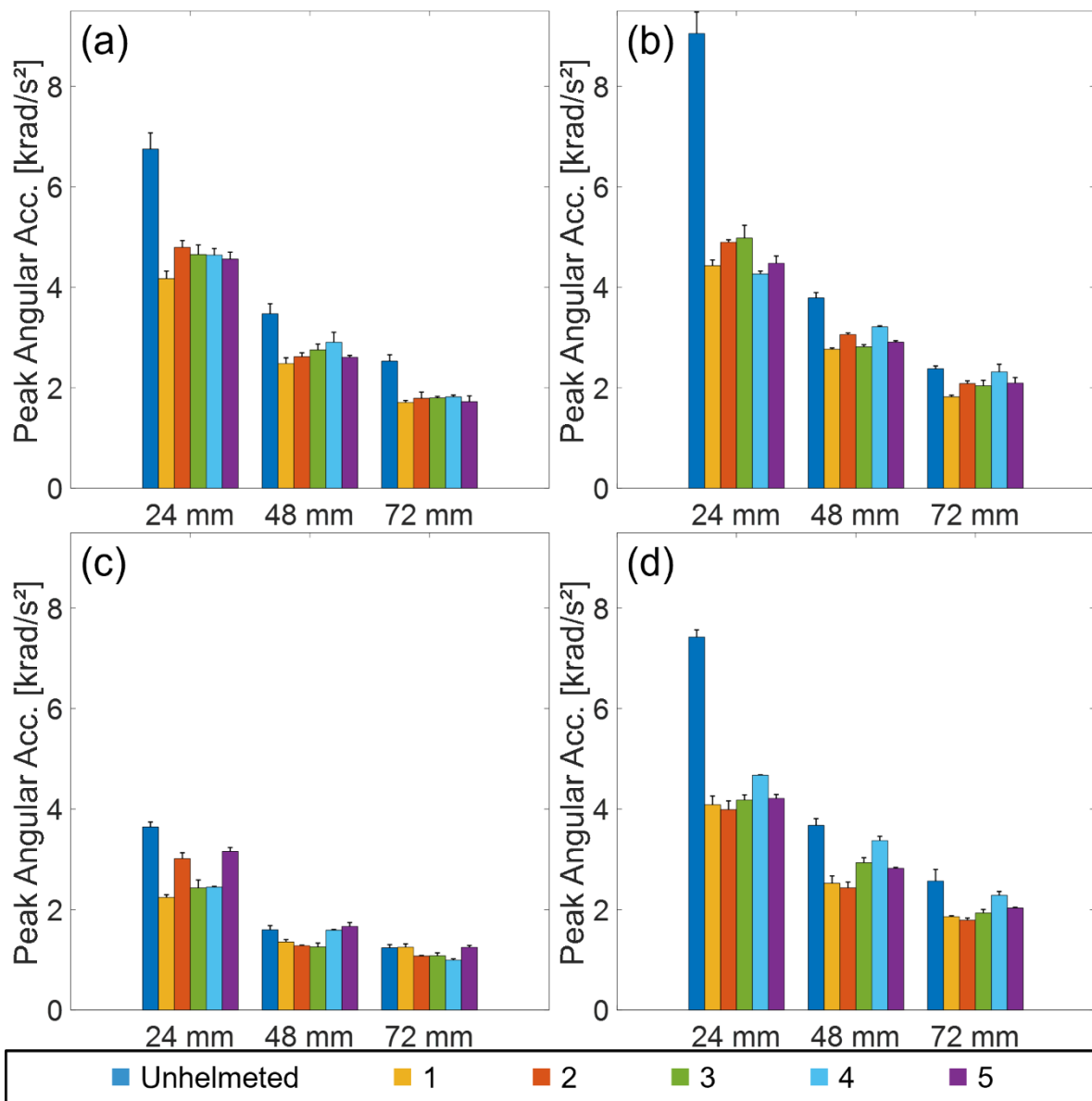


Fig. S14 Mean peak angular accelerations for all oblique surface, (a) FrontBoss, (b) RearBoss, (c) Rear, and (d) Side site impacts

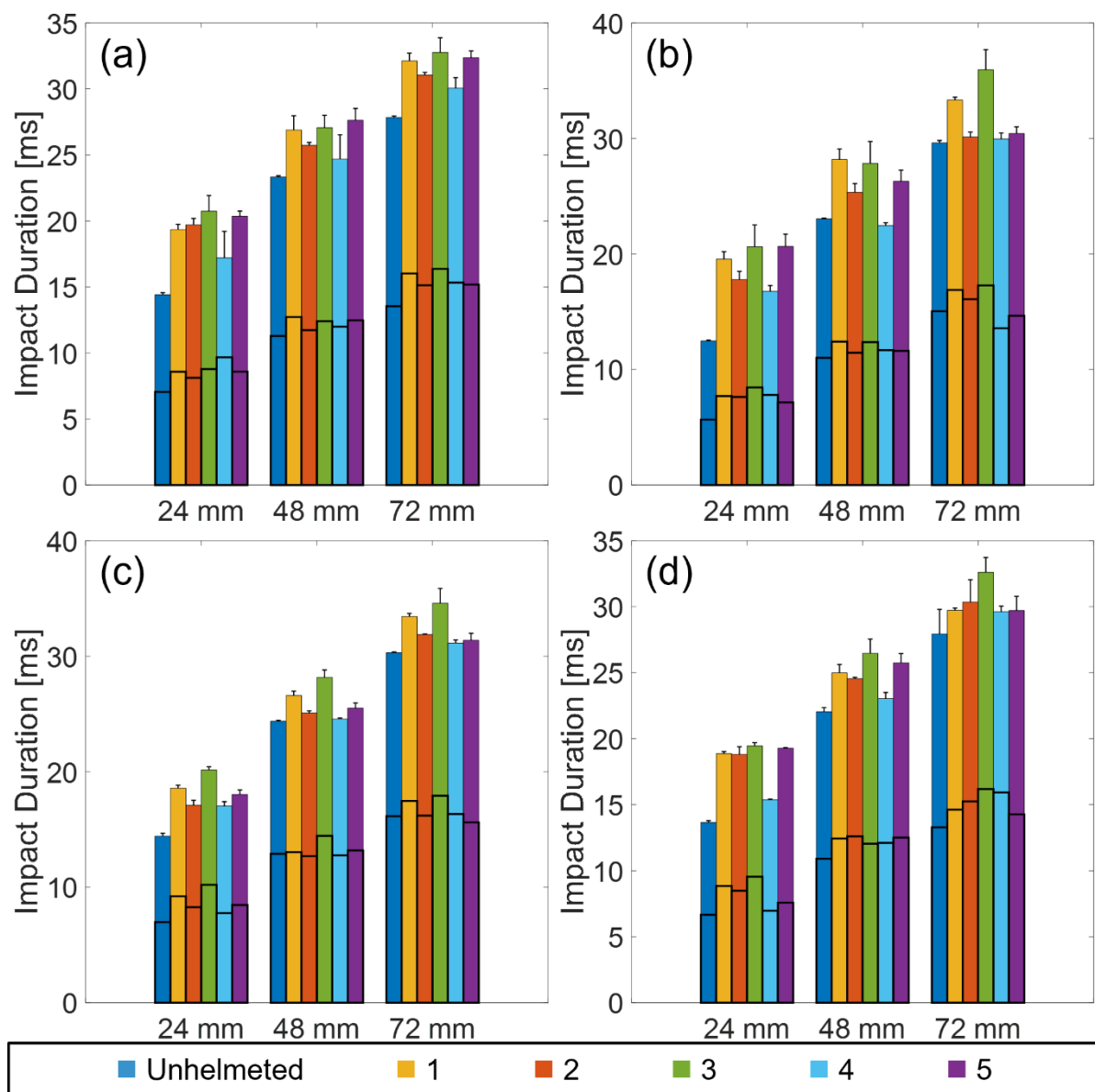


Fig. S15 Mean impact durations with horizontal bars indicating the proportion of time to peak (bottom half) and rebound time (top half) for all oblique surface, (a) FrontBoss, (b) RearBoss, (c) Rear, and (d) Side site impacts.

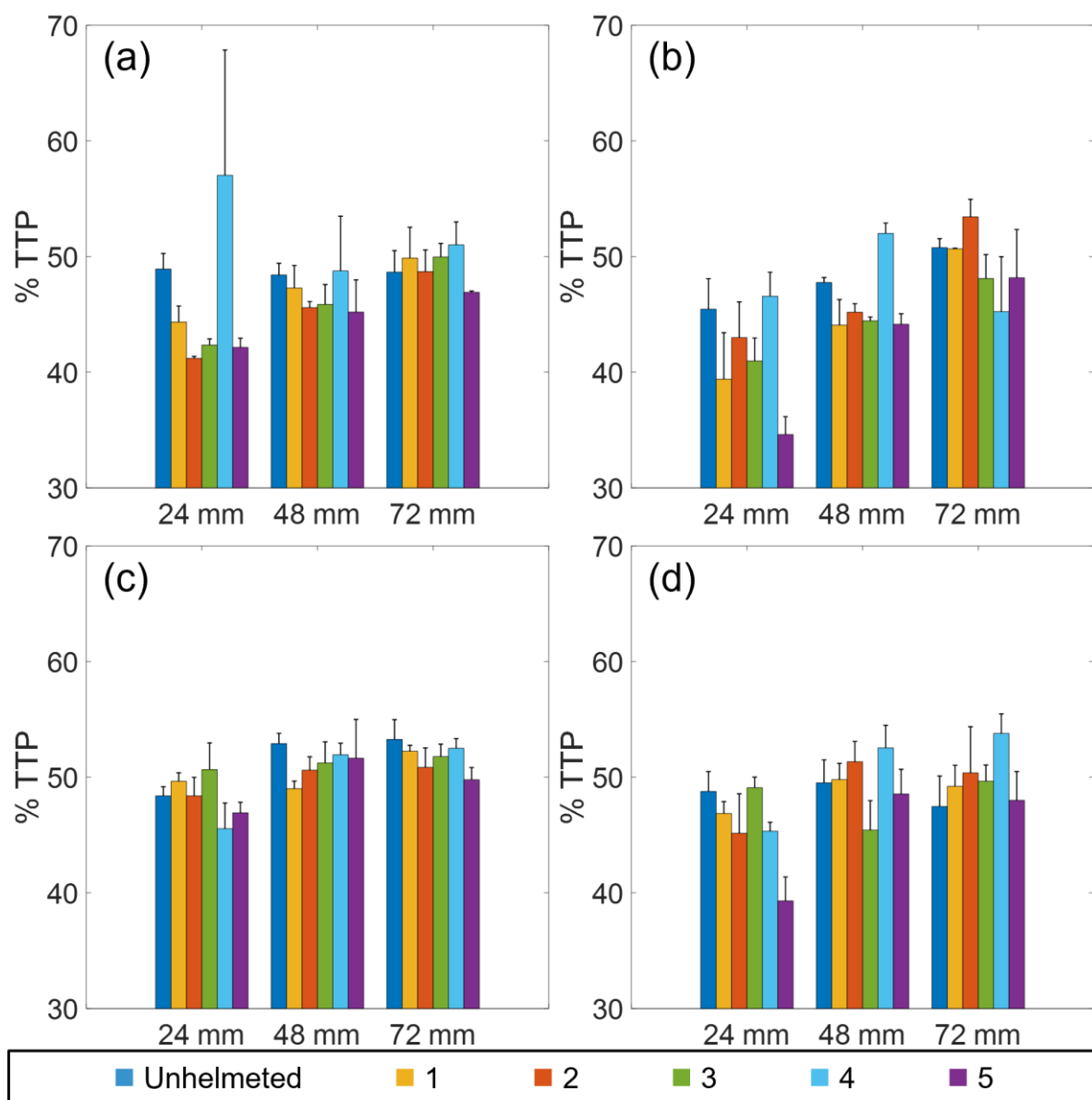


Fig. S16 Mean percentage of time to peak of the total impact duration for all oblique surface, (a) FrontBoss, (b) RearBoss, (c) Rear, and (d) Side site impacts

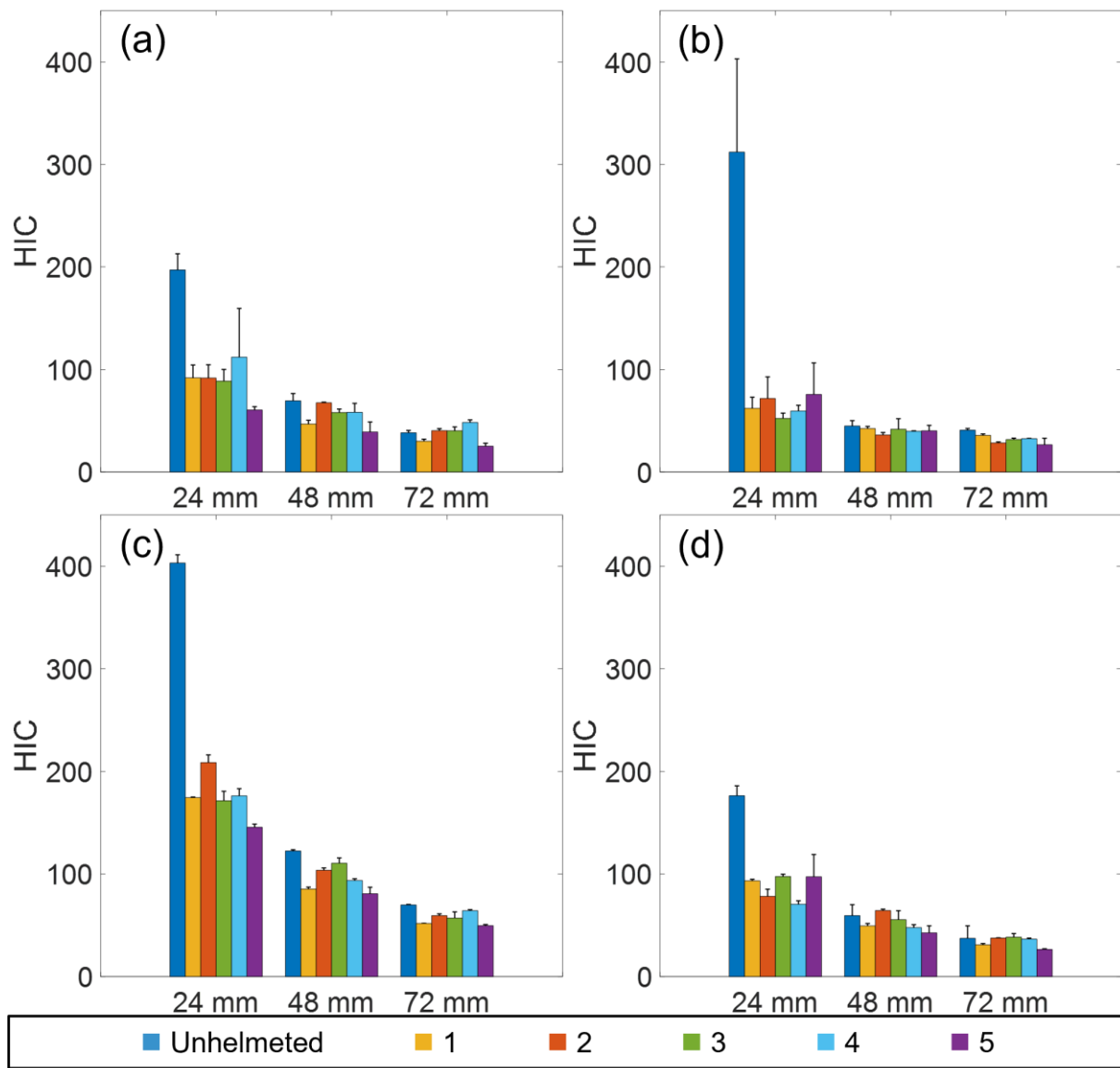


Fig. S17 Mean HIC for all oblique surface, (a) FrontBoss, (b) RearBoss, (c) Rear, and (d) Side site impacts

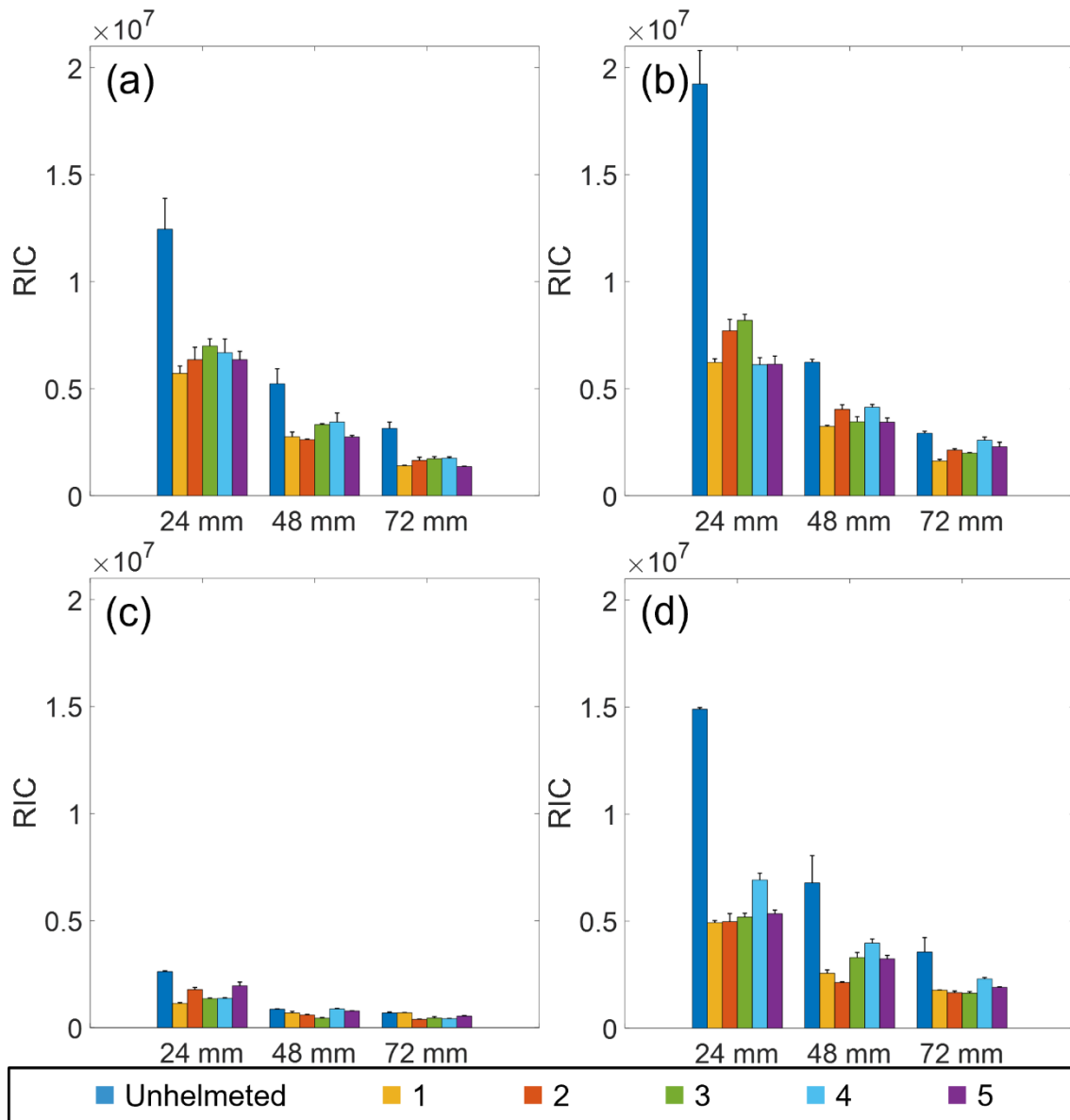


Fig. S18 Mean RIC for all oblique surface, (a) FrontBoss, (b) RearBoss, (c) Rear, and (d) Side site impacts